AGU PUBLICATIONS

Paleoceanography

RESEARCH ARTICLE
10.1002/2015PA002854

Key Points:
- Exquisitely preserved fossil foraminifera are obtained through the Tanzania Drilling Project
- Examined cores at Site 24 are biochronologically dated 99.9–95.9 Ma (early Cenomanian)
- Foraminiferal isotopic temperatures indicate a "hot greenhouse" mode during the mid-Cretaceous

Supporting Information:
- Figure S1
- Table S1
- Table S2

Correspondence to:
A. Ando,
AndoA@si.edu;
atsushi.ando@bugware.com

Citation:
Ando, A., B. T. Huber, K. G. MacLeod, and D. K. Watkins (2015), Early Cenomanian "hot greenhouse" revealed by oxygen isotope record of exceptionally well-preserved foraminifera from Tanzania, *Paleoceanography*, *30*, 1556–1572, doi:10.1002/2015PA002854.

Received 6 JUL 2015
Accepted 1 NOV 2015
Accepted article online 4 NOV 2015
Published online 30 NOV 2015

Early Cenomanian "hot greenhouse" revealed by oxygen isotope record of exceptionally well-preserved foraminifera from Tanzania

Atsushi Ando[1,2], Brian T. Huber[1], Kenneth G. MacLeod[3], and David K. Watkins[4]

[1]Department of Paleobiology, National Museum of Natural History, Smithsonian Institution, Washington, Dist. of Columbia, USA, [2]BugWare, Inc., Tallahassee, Florida, USA, [3]Department of Geological Sciences, University of Missouri, Columbia, Missouri, USA, [4]Department of Earth and Atmospheric Sciences, University of Nebraska-Lincoln, Lincoln, Nebraska, USA

Abstract The search into Earth's mid-Cretaceous greenhouse conditions has recently been stimulated by the Tanzania Drilling Project (TDP) which has recovered exceptionally well-preserved biogenic carbonates from subsurface pre-Neogene marine sediments in the eastern margin of central Africa. Published Tanzanian oxygen isotope records measured on exquisitely preserved foraminiferal tests, dating to as old as ~93 Ma, provided evidence for a Turonian "hot greenhouse" with very high and stable water-column temperatures. We have generated a comparable data set of exceptionally well-preserved foraminifera from a lower Cenomanian interval of TDP Site 24 spanning 99.9–95.9 Ma (planktonic foraminiferal *Thalmanninella globotruncanoides* Zone; nannofossil *Corollithion kennedyi* to *Lithraphidites eccentricus* Zones), thereby extending the age coverage of the Tanzanian foraminiferal $\delta^{18}O$ record back by ~7 million years. Throughout the interval analyzed, the new foraminiferal $\delta^{18}O$ data are consistently around −4.3‰ for surface-dwelling planktonic taxa and −1.9‰ for benthic *Lenticulina* spp., which translate to conservative paleotemperature estimates of >31°C at the surface and >17°C at the sea floor (upper bathyal depths). Considering the ~40°S Cenomanian paleolatitude of TDP Site 24, these estimates are higher than computer simulation results for accepted "normal" greenhouse conditions (those with up to 4X preindustrial pCO_2 level) and suggest that the climate mode of the early Cenomanian was very similar to the Turonian hot greenhouse. Taking account of other comparable data sources from different regions, the hot greenhouse mode within the normal mid-Cretaceous greenhouse may have begun by the latest Albian, but the precise timing of the critical transition remains uncertain.

1. Introduction

For decades, the mid-Cretaceous has received considerable attention as a robustly data-supported period of Earth's extensive greenhouse climate [e.g., *Barron and Washington*, 1985; *Larson*, 1991a, 1991b; *Caldeira and Rampino*, 1991; *Huber et al.*, 1995; *Johnson et al.*, 1996; *Clarke and Jenkyns*, 1999; *Poulsen et al.*, 2001]. It was relatively recently, though, that standard paleotemperature reconstructions using foraminiferal oxygen isotopes have become truly useful for the paleoclimatology of this age interval, especially since the benchmark studies of *Norris and Wilson* [1998] and *Wilson and Norris* [2001] in conjunction with the latest Cretaceous-Paleogene case study of *Pearson et al.* [2001]. These contributions focused specifically on the analyses of exquisitely preserved "glassy" foraminifera occasionally found in clay-rich sediments on siliciclastic margins. Such foraminiferal tests were taken as the archives of effectively primary $\delta^{18}O$ compositions, allowing for reasonable absolute estimates of past marine temperatures. In contrast, $\delta^{18}O$ signatures in morphologically well-preserved yet whitish, "frosty" chalk-hosted foraminifera were shown typically to be diagenetically compromised, particularly in low to middle latitude settings. These results renewed interests in mid-Cretaceous foraminiferal $\delta^{18}O$ study and led to organization of several new paleoceanographic research projects targeting fine-grained ocean margin settings worldwide [e.g., *Norris et al.*, 2002; *Wilson et al.*, 2002; *Bice et al.*, 2003; *Bornemann et al.*, 2008; *Friedrich et al.*, 2008; *Erbacher et al.*, 2011; *Huber et al.*, 2011; *MacLeod et al.*, 2013]. In accordance with this recent progress in paleoceanography, here we report on a new Cenomanian $\delta^{18}O$ data set from Tanzania Drilling Project (TDP) Site 24 that sheds new light on the marine paleotemperature evolution during the mid-Cretaceous.

One major achievement of the recent $\delta^{18}O$ studies of exquisitely preserved mid-Cretaceous foraminifera is the establishment of the Turonian as a prominent hyperthermal interval, that is, a "hot greenhouse" in the

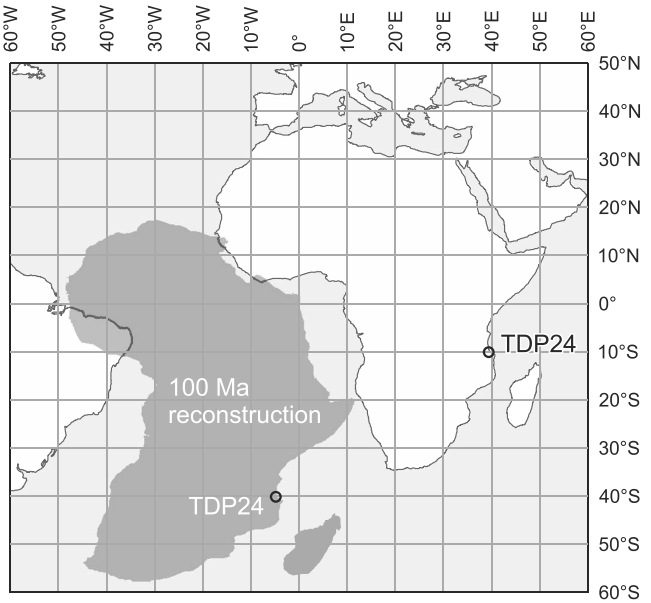

Figure 1. Map showing the present location and Cenomanian (100 Ma) paleolocation of Tanzania Drilling Project (TDP) Site 24, generated using the ODSN Plate Tectonic Reconstruction Service (http://www.odsn.de/odsn/services/paleomap/paleomap.html) [*Hay et al.*, 1999].

sense of *Huber et al.* [2002], or hothouse or supergreenhouse [*Norris et al.*, 2002; *Bice et al.*, 2003; *Bornemann et al.*, 2008]. The most recent and exceptionally detailed stable isotope data for the Turonian were reported on multiple planktonic and benthic foraminiferal taxa from TDP Sites 22 and 31 [*MacLeod et al.*, 2013; *Wendler et al.*, 2013]. These $\delta^{18}O$ data sets indicate very stable marine paleotemperatures in a Turonian southern midlatitude setting as high as 30–35°C at the surface (−4‰ to −5‰ for planktonic foraminifera) and 18–22C° at the upper slope seafloor (−1.5‰ to −2.5‰ for TDP Site 31 calcitic benthic foraminifera). Still, because of the inherently intermittent nature in the deposition of marginal siliciclastic sequences, there are significant temporal gaps in existing mid-Cretaceous $\delta^{18}O$ record from clay-hosted "glassy" foraminifera, especially for the pre-Turonian. It is noteworthy that the late Albian might also have been a period of significant warmth as inferred from the similarly low foraminiferal $\delta^{18}O$ values at Ocean Drilling Program (ODP) Sites 1050 and 1052 of Blake Nose, western North Atlantic [*Wilson and Norris*, 2001; *Petrizzo et al.*, 2008], but the relationship between the inferred Albian warming event and the Turonian hot greenhouse has not been adequately determined given the lack of reliable $\delta^{18}O$ data for the intervening Cenomanian Period.

A substantial amount of $\delta^{18}O$ measurements on exquisitely preserved Cenomanian foraminifera does exist for ODP sites at Demerara Rise, equatorial Atlantic [*Forster et al.*, 2007b; *Moriya et al.*, 2007; *Friedrich et al.*, 2008]. However, these Demerara Cenomanian $\delta^{18}O$ data sets are interpreted to have been strongly influenced by local paleoceanographic conditions including high net evaporation and the formation of hypersaline, oxygen-poor Demerara Bottom Water [*Jiménez Berrocoso et al.*, 2010a], thereby hindering a straightforward paleotemperature reconstruction. In addition, the only planktonic foraminifera available for the Demerara Rise case studies were two opportunistic species, for which depth ecologies are unpredictable [*Ando et al.*, 2010]. Another detailed set of Cenomanian stable isotope records was presented for well-preserved open-ocean assemblage of foraminifera at Blake Nose (ODP Site 1050), providing excellent constraints on the subtropical North Atlantic paleotemperature trends and planktonic evolutionary paleoecology [*Ando et al.*, 2009a, 2010]. Still, the specimens analyzed were shown to be slightly recrystallized, and the $\delta^{18}O$ values were subjected to discernible diagenetic shifts from the primary $\delta^{18}O$ baseline [*Ando et al.*, 2010].

2. Site Information, Material, and Methods

The mid-Cretaceous (Albian-Coniacian) marine strata widely distributed in the southeastern coastal surface/subsurface area of Tanzania (Figure 1) have recently been named the Lindi Formation [*Jiménez Berrocoso et al.*, 2015]. It is a sedimentary package characterized by thick accumulations of mainly fine-grained sediments deposited in an evolving passive margin basin formed through the breakup of Gondwana and rifting away of Madagascar from Africa [*Jiménez Berrocoso et al.*, 2010b]. The depositional environment has been generally interpreted as upper slope to outer shelf based on Turonian foraminiferal assemblages and sedimentological criteria [*Jiménez Berrocoso et al.*, 2010b, 2012]. This study provisionally limits the depositional setting to upper slope, taking into account new information from the planktonic foraminiferal assemblage (see section 3.1.2). The Cenomanian paleolatitude cited herein is ~40°S based

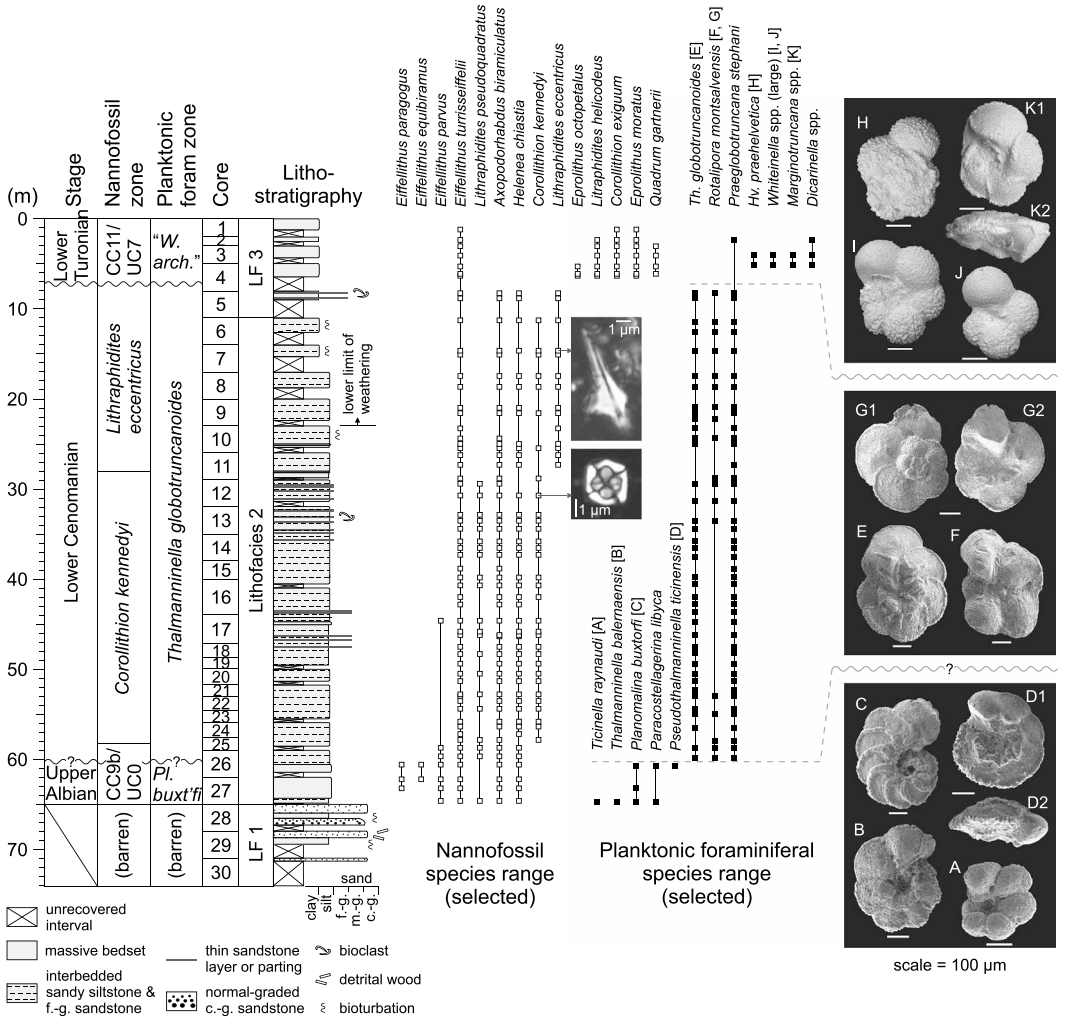

Figure 2. Summary litho- and biostratigraphy of TDP Site 24, modified from *Jiménez Berrocoso et al.* [2010b] with revised biozones and species ranges of nannofossils and planktonic foraminifera. Color photographs of Core 26, documenting the lithologic appearances across the local Albian/Cenomanian boundary (here provisionally expressed as an unconformity; see section 3.1.1), are available as Figure S1. Nannofossil zonation codes of "CC" and "UC" are based on *Perch-Nielsen* [1985] and *Burnett* [1998], respectively. Light microscopic and SEM images are for key age-diagnostic species of nannofossils and planktonic foraminifera. For planktonic foraminifera, letters A to K accompanying the listed species names correspond to those with SEM images. Sample IDs of figured specimens are as follows: A–C, sample TDP24/27/3, 62–72 cm; D, sample TDP24/26/2, 60–70 cm; E–F, sample TDP24/26/1, 67–80 cm; G, sample TDP24/8/1, 30–44 cm; H–K, sample TDP24/3/1 + 2, 93–107 cm. Abbreviations: *W. arch.*—*Whiteinella archaeocretacea*; *Hv.*—*Helvetoglobotruncana*; f.-g.—fine-grained; m.-g.—medium-grained; c.-g.—coarse-grained.

on reconstructions by *Hay et al.* [1999] and *Scotese* [2004] (Figure 1), although a slightly lower paleolatitude (~35°S) was also shown [*Sewall et al.*, 2007].

Coring at TDP Site 24 was conducted in 2007; the site was selected based on proximity to an outcrop of the Lindi Formation from which exceptionally well-preserved foraminifera of early Cenomanian age had been isolated. Drilling reached a total subsurface depth of 74 m and recovered cores representing a 65 m long sequence of dark gray siltstones underlain by coarse-grained sandstones. Initial on-site biostratigraphic study of this rock unit, based on the consistently occurring microfossils (planktonic foraminifera and nannofossils), documented a 50 m thick Cenomanian interval (Cores 24 to 4) with short intervals of Turonian sediments above and upper Albian sediments below [*Jiménez Berrocoso et al.*, 2010b].

In this study, chronostratigraphic control for this site was re-evaluated by the standard biostratigraphic analyses of planktonic foraminifera and nannofossils. For foraminifera, the same set of washed samples as

the preliminary work cited above was used (Table S1 of the supporting information). Standard smear slides for the examination of nannofossils were prepared from the different sets of raw samples (Table S2). The ranges of selected age-diagnostic species are reported herein, while the detailed assemblage characterization and taxonomy will be reported elsewhere. As described below, foraminifera and nannofossils provide the biostratigraphic results that are internally consistent at the substage level, and the new information has led to revisions of the initial interpretations on the stage boundaries and biozonation schemes of *Jiménez Berrocoso et al.* [2010b].

A total of 56 separates of the best-preserved foraminifera (all without secondary calcite infilling) were prepared for stable isotope analyses. These separates were made up of two to eight specimens (in most cases, three to six) from the 212–300 μm sieve fraction for planktonic foraminifera (*Praeglobotruncana stephani* and *Thalmanninella globotruncanoides*), and one to three large-sized specimen(s) of benthic foraminifera (*Lenticulina* spp., with a single separate of the gavelinellid gen. & sp. indet.). The most common *Lenticulina* morphotypes resembled *Lenticulina pseudosecans* or *Lenticulina secans* (17 out of 20 separates) [e.g., *Sikora and Olsson*, 1991]. Any diagenetic mineral attachments and/or diagenetically infilled final chamber(s) (see section 4) were manually removed using a sharpened needle under a stereomicroscope prior to the isotope measurements. In order to demonstrate the preservational state of our foraminiferal material, light microscopic and scanning electron microscopic (SEM) imaging were performed on selected specimens.

For analysis of stable isotope ratios in foraminifera, test calcite was reacted with "103%" phosphoric acid in a Kiel III carbonate device, and the ratios of $^{13}C/^{12}C$ and $^{18}O/^{16}O$ in the evolved CO_2 were measured on a Thermo Finnigan DeltaPlus mass spectrometer at the Biogeochemistry Isotope Laboratory, University of Missouri. Data are presented in delta (δ) notation on the Vienna PDB scale, after normalization for each run based on the difference between the within-run average of the NBS 19 standard and its recommended value ($\delta^{18}O = -2.20‰$ and $\delta^{13}C = 1.95‰$) [*Hut*, 1987]. Replicate measurements of NBS 19 prior to normalization yielded estimates of analytical precision (1 standard deviation (σ)) better than ±0.06‰ and ±0.03‰ for $\delta^{18}O$ and $\delta^{13}C$, respectively. Numerical data are listed in Table S1.

3. Biostratigraphy and Biochronology

3.1. Planktonic Foraminifera and Fundamental Chronostratigraphic Framework

3.1.1. Major Assemblage Characteristics and Stage Boundaries

Planktonic foraminifera are characterized by the assemblages of three age groups from the Albian, Cenomanian, and Turonian (Figure 2). This observation facilitates the construction of the fundamental chronostratigraphic framework with the placement of the Albian/Cenomanian (A/C) and Cenomanian/Turonian (C/T) boundaries, each delimited by a combination of the extinction of older taxa and the evolutionary appearances of younger taxa. Planktonic foraminifera are particularly important in that, by definition, the primary marker event for defining the A/C boundary is the lowest occurrence (LO) of *Th. globotruncanoides* [*Kennedy et al.*, 2004; *Ogg and Hinnov*, 2012].

The A/C boundary is placed at 60.19 m (midpoint between samples 26/2, 60–70 cm and 26/1, 67–80 cm). Across this level, the typical upper Albian planktonic foraminiferal assemblage of the *Planomalina buxtorfi* Zone (including such Albian-restricted taxa as *Pl. buxtorfi*, *Pseudothalmanninella ticinensis* (highly evolved form), *Thalmanninella balernaensis*, and *Ticinella raynaudi*) is replaced by the Cenomanian-specific taxa of the *Th. globotruncanoides* Zone (*Th. globotruncanoides* and *Rotalipora montsalvensis*). Based on this abrupt assemblage change, the local A/C boundary is here provisionally considered an unconformity, although it may be represented by a minor condensed interval as there is no definitive lithologic gap (Figure S1).

As for the C/T boundary, the same Cenomanian assemblage as above is replaced sharply by the Turonian assemblage of the "*Whiteinella archaeocretacea*" Zone across the depth of 7.25 m (midpoint of the Core 5/4 gap). The *W. archaeocretacea* Zone is an interval zone below the LO of *Helvetoglobotruncana helvetica*; note that quotation marks are used for this biozone at TDP Site 24 because *W. archaeocretacea* itself has not been identified in the washed samples. The Turonian planktonic taxa in this interval are characterized by *Helvetoglobotruncana praehelvetica* and the species of *Marginotruncana*, *Whiteinella*, and *Dicarinella*. No species indicative of the middle to upper Cenomanian, particularly the index species *Thalmanninella reicheli* and *Rotalipora cushmani*, occur. It should be noted that specimens previously identified as *R. cushmani* (Figure 2G), which was used to define the nominate zone in the initial

biostratigraphic scheme [*Jiménez Berrocoso et al.*, 2010b], are here reinterpreted as still within the evolutionary state of its ancestor *R. montsalvensis*. These observations clearly indicate that the local C/T boundary at TDP Site 24 is marked by an unconformity and that the main part of the drilled section falls solely in the lower Cenomanian *Th. globotruncanoides* Zone.

3.1.2. Planktonic Constraints on Depositional Water Depth

The planktonic foraminiferal assemblage (Figure 2) can be used to further constrain previous upper slope to outer shelf estimates for the depositional setting of the Lindi Formation, at least for the Cenomanian interval. There are three key observations: (1) predominance of the keeled taxa (*Thalmanninella* and *Praeglobotruncana*) typical for the open-ocean assemblage; (2) relatively high (~70%) planktonic abundance in the total foraminifera (Ando, unpublished data); and (3) rare but consistent occurrence of *R. montsalvensis*, for which stable isotopic paleoecology indicates a thermocline habitat [*Ando et al.*, 2009a, 2010]. In general, these conditions suggest an oceanographic setting well beyond the shelf-break front [*Hay*, 2008], which means that the Cenomanian paleobathymetric range of TDP Site 24 would likely have been limited to upper slope depths.

3.2. Nannofossils and Early Cenomanian Biochronology

3.2.1. Assemblage Characteristics

Nannofossil occurrences are biostratigraphically classified by the zonation codes of "CC" by *Perch-Nielsen* [1985] and "UC" by *Burnett* [1998] (Figure 2). The ages based on them are highly consistent with those derived from planktonic foraminifera. In the Albian part of TDP Site 24, nannofossils are of the assemblage of Subzone CC9b or Zone UC0, with *Axopodorhabdus biramiculatus* and species of the genus *Eiffellithus* (*E. equibiramus*, *E. paragogus*, *E. parvus*, and *E. turrisseiffelii*), and without *Corollithion kennedyi* or *Hayesites albianus*. The LO of *C. kennedyi*, generally used for marking the basal Cenomanian, is recognized at Sample 25/1, 23–25 cm. This level is slightly above the LO of the planktonic foraminifera *Th. globotruncanoides*. Such a stratigraphic relationship between the LOs of *Th. globotruncanoides* and *C. kennedyi* is consistent with patterns documented elsewhere [e.g., *Robaszynski et al.*, 1993; *Watkins et al.*, 2005].

The main part of the Cenomanian at TDP Site 24 can be referred to as Subzone CC9c or Zone UC 1/2 (however, see below for further discussion) with consistent occurrences of *C. kennedyi*, *Helenea chiastia*, *A. biramiculatus*, and *Lithraphidites pseudoquadratus*. Noteworthy is the entry of *Lithraphidites eccentricus* at Sample 11/2, 30–32 cm, which can be utilized for further refinement of the early Cenomanian biochronology, as detailed below. The interval from Cores 4 to 1, as with the case of planktonic foraminifera, is placed in the lower Turonian Zones CC11 or UC7 based on the sporadic occurrences of *Quadrum gartnerii*, *Eprolithus octopetalus*, *Eprolithus moratus*, *Corollithion exiguum*, and *Lithraphidites helicodeus*, together with the absence of aforementioned Cenomanian representatives.

3.2.2. Biostratigraphic Significance of *Lithraphidites eccentricus*

Lithraphidites eccentricus was first described by *Watkins and Bowdler* [1984] from a thin middle(?) Cenomanian interval at Deep Sea Drilling Project (DSDP) Site 540 (Gulf of Mexico) as a subspecies of the widely known species *L. acutus* (whose LO marks the base of Zones CC10 and UC3 [= Lower/Middle Cenomanian Substage boundary; e.g., *Burnett*, 1998]). Subsequently, *L. eccentricus* has seldom been mentioned in the literature [*Wiegand*, 1984; *Nederbragt et al.*, 2001; *Corbett et al.*, 2014].

The initial age interpretation of the middle(?) Cenomanian for the *L. eccentricus* type level was based on a co-occurring planktonic foraminiferal assemblage [*Premoli Silva and McNulty*, 1984; *Watkins and Bowdler*, 1984], which, in light of taxonomic updates since then, no longer can be used to subdivide the Cenomanian at the substage level. The presence of "*Hedbergella libyca*" [*Premoli Silva and McNulty*, 1984] [= *Paracostellagerina libyca*; e.g., *Georgescu and Huber*, 2006] is noteworthy because this morphologically distinctive taxon became extinct a while after the A/C boundary. This strongly suggests that the *L. eccentricus* type level cannot be stratigraphically as high as the middle Cenomanian; in other words, an early Cenomanian origination of *L. eccentricus* is more plausible. This view is supported by case studies from the sections with better chronostratigraphic control at Moroccan margin DSDP Site 547 [*Leckie*, 1984; *Wiegand*, 1984; *Nederbragt et al.*, 2001] and the Kalaat Senan region, central Tunisia [*Robaszynski et al.*, 1993].

We postulate that *L. eccentricus* has biostratigraphic significance as an additional datum in the early Cenomanian. Nevertheless, the proposed "*L. eccentricus* Zone" is tentative and informal. The base of the zone is definable herein by the LO of the nominate species, whereas the top depends on a rigorous taxonomic

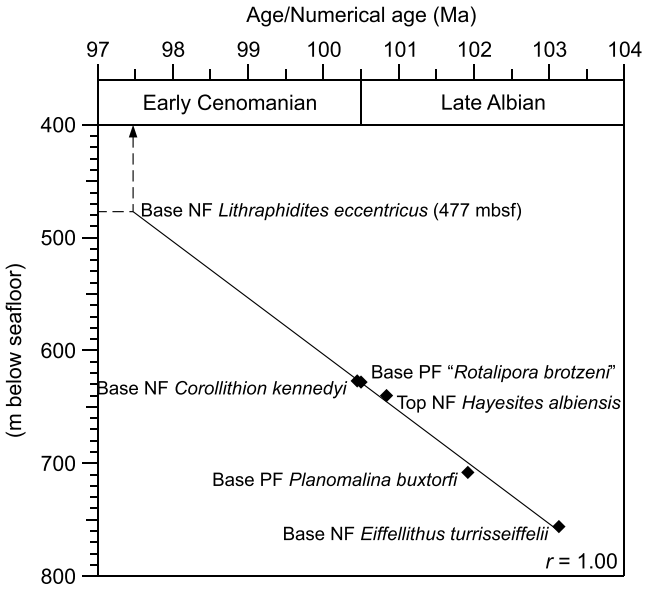

Figure 3. Age vs. depth relationship of index nannofossil and planktonic foraminiferal species across the Albian/Cenomanian boundary at DSDP Site 547, Moroccan Margin [*Nederbragt et al.*, 2001, Figure 2 therein]. This diagram is used to derive 97.5 Ma for the first appearance datum of *Lithraphidites eccentricus*. In the range chart of *Nederbragt et al.* [2001], taxon name *Lithraphidites acutus* is used, but it should refer to the subspecies *eccentricus*, judging from their Plate 3.16 as well as from another nannofossil biostratigraphic study by *Wiegand* [1984]. "*Rotalipora brotzeni*" is probably attributed to *Thalmanninella globotruncanoides* in the recently updated taxonomic scheme. Abbreviations: NF—nannofossil; PF—planktonic foraminifera.

distinction between *L. eccentricus* and *L. acutus*. Accordingly, the use of conventional CC and/or UC zonal coding cannot be justified for the *L. eccentricus* Zone. This treatment further affects the usage of Zone CC9c or UC1/2, and hence, we use the *C. kennedyi* Zone for clarity (Figure 2).

3.2.3. Numerical Age Model

A numerical age estimate of the LO of *L. eccentricus* is possible using biostratigraphic data from DSDP Site 547 [*Nederbragt et al.*, 2001], where a series of important bioevents are recognized across the A/C boundary. As graphically shown in Figure 3, the datum point of 97.5 Ma is derived using a linear extrapolation of the age vs. depth plots on the Geologic Time Scale 2012 calibrations [*Ogg and Hinnov*, 2012].

The Cenomanian chronology for TDP Site 24 is constructed by a simple linear relationship of the two first appearance datums of *C. kennedyi* (100.45 Ma) [*Ogg and Hinnov*, 2012] at 58.28 m and *L. eccentricus* (97.5 Ma; this study) at 28.07 m. The calculated sedimentation rate is 1.02 cm/kyr. Application of this age-depth relationship allows for numerical age scaling of the isotopically analyzed interval at 99.9–95.9 Ma. This nannofossil biochronology corroborates the independently derived early Cenomanian age from planktonic foraminiferal biostratigraphy.

4. Foraminiferal Preservation

While many of the Cenomanian foraminiferal specimens from TDP Site 24 are infilled by secondary calcite, it is often possible to collect unfilled, excellently preserved specimens that are present in small proportions in Cores 21 to 6. Two species of keeled planktonic foraminifera *Pg. stephani* and *Th. globotruncanoides* are found to allow for consistent selection of specimens in such exquisite preservation for stable isotopic analyses. For benthic foraminifera, it is interesting to note that taxon-specific diagenesis seems to exist. The ubiquitous calcareous trochospiral taxa such as *Gyroidinoides* and the gavelinellids (*Gavelinella*, *Berthelina*, etc.), most widely used in previous stable isotopic studies, are found to be totally infilled in nearly all of the samples examined, a lone exception for which is an unfamiliar gavelinellid taxon (gen. & sp. indet.) in only one sample. On the other hand, specimens of *Lenticulina* often exhibit excellent preservation. The almost exclusive use of *Lenticulina* spp. for this study is due to this taphonomic bias.

The selected specimens for stable isotope analysis are exceptionally well preserved, with the presence of minor, if any, secondary calcite that is volumetrically too small to influence the primary stable isotopic signatures (Figure 4). Specifically, the specimens observed under a light stereomicroscope are characterized by hollow tests, complete translucency of the keels (for two planktonic taxa) and of the umbo and limbate sutures (for *Lenticulina* spp.), and a reflective appearance of the outer wall surface. The selected specimens are also observed to have a subtle whitish opacity on chamber walls (Figures 4b–4d). Examination of the wall cross section by SEM confirms excellent preservation of internal test ultrastructures, which are the microlayering and microgranular texture of planktonic foraminifera (Figures 4e and 4f), and the prismatic structure of *Lenticulina* spp. (Figure 4g). On the other hand, subtle submicron-scale euhedral calcite is usually present

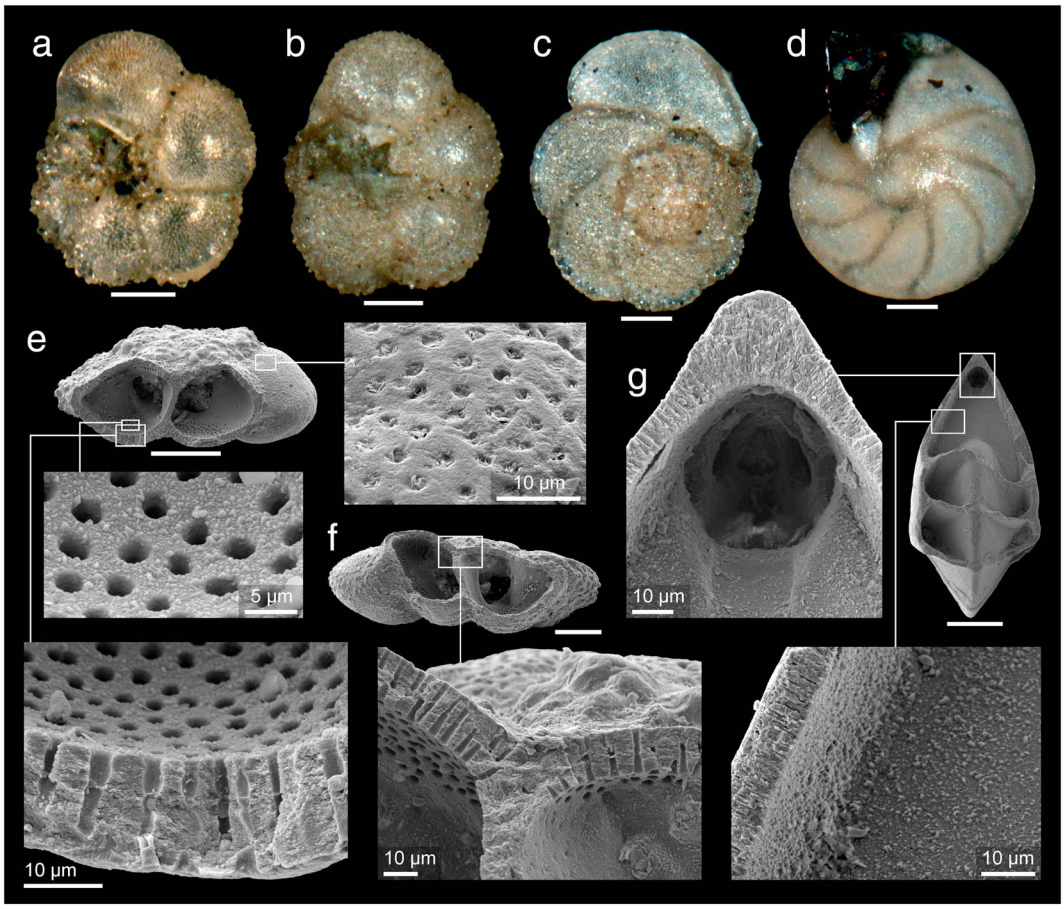

Figure 4. Light microscopic and SEM images documenting preservational states of foraminiferal specimens analyzed. Scale bar lengths for whole specimen views are 100 μm, and those for all others are specified. (a) *Praeglobotruncana stephani* (sample TDP24/15/1, 66–81 cm), example of exceptional best-preserved specimen with fully translucent test. (b) *Pg. stephani* (sample TDP24/15/3, 30–50 cm), very well preserved specimen with glauconite(?) umbilical infilling. (c) *Thalmanninella globotruncanoides* (sample TDP24/15/3, 30–50 cm), very well preserved specimen. (d) *Lenticulina* sp. (sample TDP24/15/3, 30–50 cm), very well preserved specimen with translucent umbo and limbate sutures but whitish chamber wall, and pyritized ultimate chamber. (e) Dissected specimen of *Pg. stephani* (sample TDP24/21/1, 85–97 cm) with magnified views of wall cross section and chamber interior as well as chamber exterior surfaces. Note that primary wall ultrastructures (microlayering and microgranular texture) are perfectly preserved, yet chamber interior surface is attached by subtle secondary euhedral calcite, and the outer surface may be covered by thin cortex partly plugging pore inlets. (f) Dissected specimen of *Pg. stephani* (sample TDP24/15/3, 30–50 cm) with magnified view of wall cross section and chamber interior. Note the preservation of microlayering and microgranular texture. (g) Dissected specimen of *Lenticulina* sp. (sample TDP24/15/3, 30–50 cm) with magnified views of wall cross section and chamber interior. Note the preservation of primary prismatic structure and pores, but minor attachments of secondary euhedral calcite on the chamber interior surface.

on the interior chamber surfaces (Figures 4e and 4g), which may explain the somewhat whitish chamber walls under reflected light. The pore inlets are cleanly open, but those of the planktonic taxa are often plugged by a thin material of unknown composition (possibly a primary biological feature) covering the outer surface (Figure 4e).

In addition to the above, it is commonly observed in the examined samples that planktonic foraminifera are developed by a glauconite-like greenish-gray mineral in the umbilical area and/or within the last chamber(s) (Figure 4b) and that *Lenticulina* spp. have pyritized last one or two chambers (Figure 4d). Although the diagenetic mechanisms are unknown, these observations are indicative of certain taphonomic processes unique to each of these taxonomic groups.

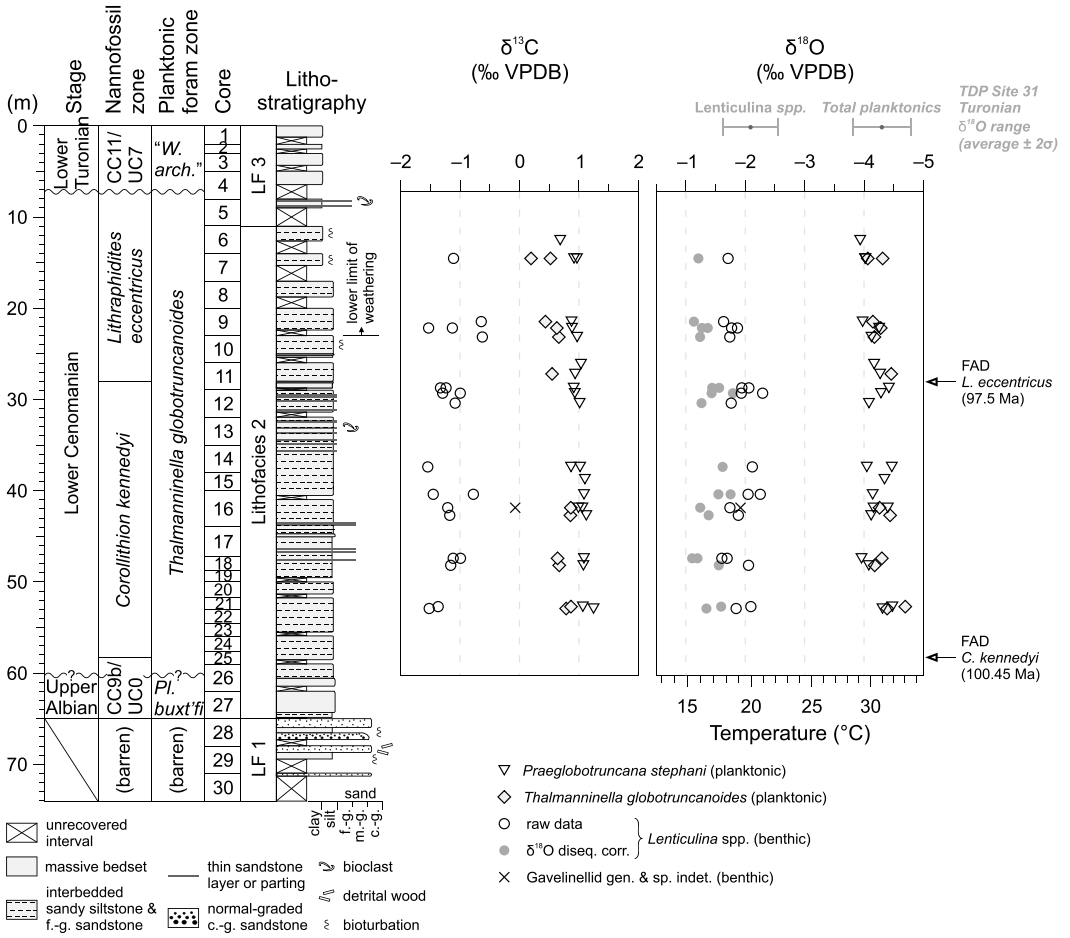

Figure 5. Stable isotope ($\delta^{18}O$ and $\delta^{13}C$) data measured on exceptionally well-preserved foraminifera at TDP Site 24. Paleotemperature scale at the bottom of $\delta^{18}O$ panel, which applies to both planktonic and benthic foraminifera at this site, is based on the equation of *Kim and O'Neil* [1997] with the assumption of a mean seawater $\delta^{18}O$ value of $-1‰_{SMOW}$ (see section 5.1.3). In addition to raw $\delta^{18}O$ data of *Lenticulina* spp., their disequilibrium-corrected (diseq. corr.) $\delta^{18}O$ values are also plotted, by adding +0.5‰ (see section 5.1.2). The Turonian $\delta^{18}O$ ranges of TDP Site 31 are calculated from *MacLeod et al.* [2013]: "*Lenticulina* spp." is based on all $\delta^{18}O$ data from this group (i.e., not only *Lenticulina* spp. but also *Lenticulina* sp. 1 and sp. 2); "Total planktonics" are based on $\delta^{18}O$ data from all planktonic foraminifera except for the heterohelicids. Abbreviations: VPDB—Vienna Peedee belemnite; FAD—first appearance datum.

5. Stable Isotopic Results

5.1. Oxygen Isotopes

5.1.1. Planktonic and Benthic $\delta^{18}O$ Characteristics

The lower Cenomanian $\delta^{18}O$ values generated from exceptionally well-preserved foraminifera are remarkably consistent and invariant for each taxon analyzed (Figure 5). The planktonic $\delta^{18}O$ values of *Pg. stephani* and *Th. globotruncanoides* are inseparable and cluster at $-4.2 \pm 0.3‰$ ($n = 22$) and $-4.4 \pm 0.4‰$ ($n = 13$), respectively (error = 2σ). The benthic $\delta^{18}O$ values of *Lenticulina* spp. are also highly stable at $-1.9 \pm 0.4‰$ ($n = 20$). The gavelinellid (gen. & sp. indet.) specimen provides a single data point of $\delta^{18}O = -1.9‰$.

The marked isotopic contrast between planktonic and benthic $\delta^{18}O$ values is a predictable consequence of the temperature-dependent oxygen isotope fractionation and the water-column temperature gradient. Namely, as the temperature of ambient water increases, the $\delta^{18}O$ values of biogenic calcite decrease due to the physicochemical processes regulating the behavior of oxygen isotope species during calcification. Thus, planktonic foraminifera inhabiting in the warm upper ocean always have lower $\delta^{18}O$ values than benthic foraminifera that live in the cooler bottom water.

5.1.2. Disequilibrium $\delta^{18}O$ Correction for *Lenticulina* spp.

The benthic *Lenticulina* group has a great potential in $\delta^{18}O$-based paleoceanography in that the test sizes and mass are often large enough for single-specimen analysis on state-of-the-art isotope-ratio mass spectrometers and that the robust tests are more resistant to diagenesis than other common benthic taxa. For this potential to be realized, though, any offset due to biologically induced isotope disequilibrium (so-called "vital effects") should be known and adjustable. Such disequilibrium $\delta^{18}O$ offsets of Cretaceous *Lenticulina* spp. (or the nodosariids) were found and/or discussed by *Barrera et al.* [1987], *Fassell and Bralower* [1999], and *Friedrich et al.* [2006]. More recently, *Wendler et al.* [2013] presented by far the most detailed and stratigraphically comprehensive $\delta^{18}O$ records of *Lenticulina* spp. in Turonian TDP Site 31, showing highly consistent $\delta^{18}O$ values without significant intra- and inter-species $\delta^{18}O$ differences. In their whole benthic $\delta^{18}O$ data set, a constant offset by ~+0.5‰ was apparent for *Lenticulina* spp. against values from the majority of co-occurring gavelinellids (called "Group II"). *Wendler et al.* [2013] determined that the $\delta^{18}O$ data from Group II taxa reliably approximate the equilibrium calcite $\delta^{18}O$ value with respect to the ambient bottom water. This conclusion has been supported by the measurements on coexisting *Oridorsalis* [*Wendler et al.*, 2013], a taxon recognized to have been most useful with no disequilibrium $\delta^{18}O$ offset for Cenozoic paleoceanography [*Katz et al.*, 2003] and also for a Santonian-Campanian case study [*Ando et al.*, 2013].

Due to the demonstrated reliability in calibration of the isotope disequilibrium effect as discussed above, we apply a $\delta^{18}O$ correction factor of +0.5‰ to adjust our lower Cenomanian *Lenticulina* $\delta^{18}O$ data from TDP Site 24. We can add confidence to this approach because of the exceptional test preservation of foraminifera as well as the similarity in age, paleogeography, and depositional setting between Turonian TDP sites studied by *Wendler et al.* [2013] and TDP Site 24.

5.1.3. Paleotemperature Reconstruction

5.1.3.1. General

The $\delta^{18}O$ temperature scale applied in Figure 5 is based on the *Kim and O'Neil* [1997] equation, reformulated by *Bemis et al.* [1998, Table 1] in the following form of:

$$T\,(^{\circ}\mathrm{C}) = 16.1 - 4.64 \times \left(\delta^{18}O_{calcite} - \delta^{18}O_{water}\right) + 0.09 \times \left(\delta^{18}O_{calcite} - \delta^{18}O_{water}\right)^2.$$

Given the reasonable assumption that continental ice sheets did not exist during the Cenomanian (see later discussion), we use a mean seawater $\delta^{18}O$ value of $-1‰_{SMOW}$ for an ice-free world [*Shackleton and Kennett*, 1975] (SMOW—Standard Mean Ocean Water), which corresponds to $-1.27‰$ for $\delta^{18}O_{water}$ in the equation [*Hut*, 1987; *Grossman*, 2012; *Pearson*, 2012]. For this study, we assume that the same $\delta^{18}O_{water}$ value is applicable for both planktonic and benthic foraminiferal $\delta^{18}O$ data. In this case, the estimated Cenomanian marine paleotemperatures are ~31°C for the upper ocean (i.e., $\delta^{18}O_{calcite} = -4.3‰$ from planktonics) and ~17°C for the bottom water ($\delta^{18}O_{calcite} = -1.9 + 0.5 = -1.4‰$ from benthic *Lenticulina* spp.). Ideally, the use of $\delta^{18}O$ in foraminiferal calcite for quantitative paleotemperature reconstructions would also take account of additional effects on past seawater and/or foraminiferal $\delta^{18}O$ compositions, such as evaporation-precipitation balance, latitudinal sea-surface $\delta^{18}O$ gradient, riverine freshwater input, seawater pH, and, in a strict sense, the oceanic $\delta^{18}O$ evolution on geologic timescales. However, these variables are difficult to constrain precisely.

Below, we evaluate the above mentioned assumptions and issues related to paleotemperature reconstructions in some detail. Nonetheless, our contention is that the simple calculation outlined above provides a sufficiently good approximation of marine paleotemperatures for this study, which may be somewhat underestimated but are never overestimated.

5.1.3.2. Paleotemperature Equation

The widely known paleotemperature equations were thoroughly reviewed by *Grossman* [2012] and *Pearson* [2012]. The latter author pointed out that the synthetic calcite calibration of *Kim and O'Neil* [1997] provides the only available equation for temperatures as high as 40°C. This high calibration limit justifies the use of that equation for reconstructions of past extremely warm marine temperatures [*Pearson*, 2012; *Aze et al.*, 2014]. In the case of equation (1) of *Bemis et al.* [1998] derived from cultured *Orbulina universa* (at low light condition ≈ minimal symbiont activity), it has been commonly cited for the studies in mid-Cretaceous foraminiferal $\delta^{18}O$-based paleotemperatures [e.g., *Wilson and Norris*, 2001; *Norris et al.*, 2002]. However, this equation's narrower calibration range (15–25°C), and hence its dependence on linear extrapolation for higher temperatures at $>>$25°C, reduces its applicability. Note, though, that both *Kim and O'Neil* [1997] and *Bemis et al.*

[1998] equations yield almost identical paleotemperatures for our TDP Site 24 data (e.g., 30.99°C and 31.04°C, respectively, for $\delta^{18}O = -4.3‰$ at the surface).

5.1.3.3. Mean Seawater $\delta^{18}O$

The assumption that a mean seawater $\delta^{18}O$ value of $-1‰_{SMOW}$ applies to an ice-free Earth was first proposed by *Shackleton and Kennett* [1975] using a simple mass balance calculation [see also *Pearson*, 2012, p. 14]. This estimate has been accepted widely in $\delta^{18}O$-based paleoceanographic studies for the Cretaceous-Paleogene period. However, it has also been known that the pre-Cretaceous marine $\delta^{18}O$ data generated from low-Mg biogenic calcite (mainly brachiopods) are generally very low, yielding too high temperatures if a seawater $\delta^{18}O$ value of $-1‰_{SMOW}$ is used in the common equations [e.g., *Grossman*, 2012]. Specifically, a large, Phanerozoic-scale compilation of published marine $\delta^{18}O$ data has illustrated a linearly increasing trend in $\delta^{18}O$ of global seawater at a rate of ~+1‰/100 Myr, possibly reflecting Earth's tectonics and geochemical cycles [e.g., *Veizer et al.*, 1999; see also *Jaffrés et al.*, 2007]. This inferred long-term shift of seawater $\delta^{18}O$ baseline would be large enough to overestimate Cretaceous $\delta^{18}O$-based marine paleotemperatures by up to +4°C and was used by some researchers in interpreting or adjusting the relevant $\delta^{18}O$ data [e.g., *Veizer et al.*, 2000; *Wallmann*, 2004; *Royer et al.*, 2004; *Cramer et al.*, 2011]. Interestingly, with further accumulation of numerous $\delta^{18}O$ measurements, it has increasingly become obvious that the Phanerozoic seawater $\delta^{18}O$ trend fits a quadratic function, which levels off from the Cretaceous through the present [*Veizer and Prokoph*, 2015]. Therefore, it seems that a correction due to geologic ocean $\delta^{18}O$ evolution is not necessary for global Cenomanian seawater.

5.1.3.4. Latitudinal Surface $\delta^{18}O$ Gradient

Upper ocean $\delta^{18}O$ compositions, in contrast to those of intermediate to deep waters, are known to display a systematic latitudinal gradient due to oxygen isotope fractionation accompanying water evaporation-precipitation and poleward vapor convection, that is, a Rayleigh distillation process. If an empirical latitude-dependent $\delta^{18}O$ correction is applied [*Zachos et al.*, 1994], the estimated surface paleotemperature would be ~2°C higher at the 40°S Cenomanian paleolatitude of the Tanzanian margin. In contrast to such a blanket correction scheme, recent simulations using "isotope-enabled" general circulation models (GCMs) for the distribution of surficial marine $\delta^{18}O$ compositions during the Cenomanian [*Zhou et al.*, 2008] and the early Eocene [*Tindall et al.*, 2010; *Roberts et al.*, 2011] predicted marked $\delta^{18}O$ heterogeneity without obvious latitude dependency in restricted oceanic domains. The GCM simulations by *Zhou et al.* [2008] and *Roberts et al.* [2011], in particular, predicted that Cenomanian or Eocene seawater $\delta^{18}O$ compositions off ancient Tanzania would have been close to the global mean. Thus, for simplicity, we do not apply any latitudinal corrections for TDP Site 24 planktonic $\delta^{18}O$ data.

5.1.3.5. Riverine Freshwater Input

Another potential source of uncertainty in surface seawater $\delta^{18}O$ composition is the influx of isotopically light river water. However, the effect of continental runoff is intuitively insignificant in our planktonic $\delta^{18}O$ data. Besides the open-ocean nature of the Cenomanian planktonic foraminiferal assemblage, a minimal freshwater influence on the generally low $\delta^{18}O$ values for TDP Site 24 is supported by the absence of great rivers discharging from the eastern part of Africa, a sufficiently large distance to the Cretaceous paleoshoreline (at least 70 km; *Kent et al.* [1971]) and a relatively narrow continental shelf at that time [*Sewall et al.*, 2007]. Additionally, although meteoric water in the midlatitude region should have relatively low $\delta^{18}O$ values, the Rayleigh distillation process would likely have been moderated in the greenhouse world. That is, recent GCM simulations predicted an expansion of the subtropical zone and a lesser degree of latitudinal/altitudinal $\delta^{18}O$ fractionation in precipitation, while maintaining the precipitation-evaporation-runoff balance [*Zhou et al.*, 2008; *Roberts et al.*, 2011].

In the modern surface ocean ~100 km off Tanzania (~9°S), the total range of multi-year salinity fluctuations is small (0.6 unit), indicating little or no effects of riverine freshwater forcing [*Birch et al.*, 2013]. Taking an example of a modern midlatitude salinity-$\delta^{18}O$ relationship at the northwestern Gulf of Mexico margin, a salinity change by 0.6 unit causes only 0.1‰ $\delta^{18}O$ shift even in such a highly susceptible region to freshwater dynamics with substantial water discharge from the Mississippi River and its tributaries ($\delta^{18}O_{water} = -7‰$) onto a broad, low-gradient continental shelf [*Kendall and Coplen*, 2001; *Wagner and Slowey*, 2011; *Strauss et al.*, 2012]. Compared to this modern setting, freshwater-induced $\delta^{18}O$ anomaly in mid-Cretaceous surface seawater off Tanzania, assuming similar <1 unit salinity variations, would have been even smaller in light of the above considerations on paleogeography and GCM greenhouse paleohydrology. This exercise leads us to conclude that the effect of freshwater runoff is too small to be detected in the Cenomanian planktonic $\delta^{18}O$ record of TDP Site 24.

5.1.3.6. pH

The effect of seawater pH on foraminiferal stable isotopes has recently been a topic of wide interest since the experimental work of *Spero et al.* [1997]. Using a physicochemical basis for oxygen isotope fractionation between different species of dissolved inorganic carbon (DIC), *Zeebe* [2001] advocated that a pH-induced $\delta^{18}O$ shift in marine carbonates must be considered, especially under past high-CO_2 conditions, at −1.42‰ per pH unit. Some researchers have applied pH corrections to foraminiferal $\delta^{18}O$ data [e.g., *Royer et al.*, 2004; *Cramer et al.*, 2011; *Aze et al.*, 2014], but they used different approaches. For the Cretaceous, modeled secular pH variations show significant discrepancies between case studies [e.g., *Wallmann*, 2004; *Zeebe*, 2012]. Meanwhile, a recent culture experiment demonstrated that foraminifera can regulate pH internally during chamber calcification [*de Nooijer et al.*, 2009]; if this is the case, a pH-related $\delta^{18}O$ shift in foraminiferal tests cannot be viewed as a purely physicochemical process. Given these uncertainties, it is premature to apply a pH correction as a common practice in foraminiferal $\delta^{18}O$-based paleoceanography. Instead, we note that the reconstructed Cenomanian surface- and bottom-water paleotemperatures may be underestimated, for example, by up to +3°C (equates to ~−0.7‰ shift of $\delta^{18}O$ in foraminifera) assuming a possible lowering of pH units by 0.5 under mid-Cretaceous high-pCO_2 conditions [*Zeebe*, 2001, 2012].

5.2. Carbon Isotopes

Of the taxon-specific Cenomanian foraminiferal $\delta^{13}C$ records from TDP Site 24 (Figure 5), the most densely measured are for the planktonic foraminifera *Pg. stephani*, whose data show remarkable consistency averaging 1.2 ± 0.3‰ ($n = 22$; error = 2σ) with a subtle gradual shift toward lower values up-section. The $\delta^{13}C$ values of *Th. globotruncanoides* average at 0.8 ± 0.6‰ ($n = 13$), representing a small negative offset from the *Pg. stephani* values. Compared to the planktonic data, $\delta^{13}C$ values of *Lenticulina* spp. display greater scatter at −1.4 ± 0.6‰ ($n = 20$). The single data point of the gavelinellid (gen. & sp. indet.) at −0.1‰ falls between the $\delta^{13}C$ data clusters of the two planktonic species and *Lenticulina* spp.

The observed inter-taxon $\delta^{13}C$ offsets are understood in terms of known mechanisms in foraminiferal paleoecology. For symbiont-free Cretaceous planktonic taxa, there are two main factors controlling their $\delta^{13}C$ compositions, of which one is species-specific depth habitats (i.e., surface-dwelling taxa have higher $\delta^{13}C$ values than deeper dwelling taxa, reflecting water-column $\delta^{13}C$ gradient in DIC) and another is seasonality (e.g., summer surface dwellers have the highest $\delta^{13}C$ values via the seasonal photosynthetic upper ocean ^{13}C enrichment in DIC) [e.g., *Ando et al.*, 2010]. The relationship of $\delta^{13}C$ distributions between *Pg. stephani* and *Th. globotruncanoides* is similar to the case of a coeval western North Atlantic assemblage [*Ando et al.*, 2010]; if that paleoecological model is applicable to the Tanzanian assemblage, *Pg. stephani* is considered as a summer surface dweller and *Th. globotruncanoides* as a spring surface dweller.

The $\delta^{13}C$ values of benthic foraminifera are thought to largely reflect their within-sediment microhabitat preferences, in addition to possible species-specific vital effects of carbon isotope disequilibrium. In general, tests of calcitic trochospiral gavelinellids faithfully reflect the $\delta^{13}C$ composition of DIC in ambient bottom water. Thus, the single gavelinellid data point of $\delta^{13}C = -0.1$‰ could potentially be the reference $\delta^{13}C$ value of the Cenomanian Tanzanian equilibrium calcite at the seafloor. Compared to this, the significantly lower $\delta^{13}C$ values of *Lenticulina* spp. are interpreted as reflecting its deep infaunal habitat. Living below the sediment-water interface, test formation of *Lenticulina* would have occurred under the influence of interstitial water in which DIC is imprinted by organic matter remineralized in the sediment column. An alternative explanation would be incorporation of metabolic CO_2 into the tests [*Wendler et al.*, 2013].

In terms of carbon isotope stratigraphy, the lack of obvious shifts in the $\delta^{13}C$ profile of *Pg. stephani* suggests that the age interval during which deposition of the examined portion of TDP Site 24 occurred should have spanned a non-event period of the secular $\delta^{13}C$ trend. This observation strengthens the proposed early Cenomanian age by means of calcareous microfossil biochronology, because this age interval is established to have been a time of fairly invariant $\delta^{13}C$ composition in seawater [e.g., *Mitchell et al.*, 1996; *Ando et al.*, 2009a]. One notable difference from previous studies is that the early Cenomanian $\delta^{13}C$ baseline is at 1‰ for Tanzanian planktonic foraminifera (Figure 5), whereas it is at ~2‰ for coeval bulk carbonates or isolated planktonic foraminifera elsewhere. This observation might be of interest in light of the past global $\delta^{13}C$ distribution of oceanic DIC. In this regard, although $\delta^{13}C_{DIC}$ in the surface ocean is generally considered homogenous, modern observational data detected the surface seawater off East Africa as possessing noticeably low $\delta^{13}C$ composition relative to the global mean [*Gruber and Keeling*, 2001].

6. Discussion

6.1. Tanzanian $\delta^{18}O$ Evidence for Cenomanian Hot Greenhouse

The reconstructed early Cenomanian marine paleotemperatures of >31°C at the surface and >17°C at the seafloor (upper slope) are notably high at the ~40°S paleolatitude for TDP Site 24. These estimates are close to, but generally above, the temperatures in the modern tropics and are far greater than the present-day temperatures at 40°S off Africa where the annual ranges are 16°C at the surface and 12–9°C at 200–500 m depth (World Ocean Atlas 2009; http://www.nodc.noaa.gov/OC5/WOA09/pr_woa09.html). When compared to the GCM simulations for mid-Cretaceous and Paleogene greenhouse climates with 4X or 8X preindustrial pCO_2 levels [*Zhou et al.*, 2008; *Roberts et al.*, 2011], our conservative estimate of >31°C surface paleotemperatures still well exceeds model predictions for 40°S paleolatitude and is consistent with the result of an extreme pCO_2 simulation with >4500 ppm [*Bice et al.*, 2003].

Our new TDP Site 24 $\delta^{18}O$ data from exceptionally well-preserved foraminifera can be reasonably interpreted as evidence for a hot greenhouse climate during the early Cenomanian. The $\delta^{18}O$ ranges of both planktonic and benthic foraminifera are nearly identical to those of the pre-established Turonian hot greenhouse at nearby TDP sites (Figure 5). This finding will help clarify previous views on Cenomanian paleoclimates that have been more or less controversial. That is, the Cenomanian has generally been characterized as a period of extensive greenhouse conditions, but this view was often challenged by combining indirect lines of evidence for the existence of continental ice sheets, namely, a presumed (glacio)eustatic control on the development of marine sedimentary sequences, and short-term marine $\delta^{18}O$ and faunal shifts indicative of cooling [e.g., *Gale et al.*, 2002, 2008; *Miller et al.*, 2003, 2005; *Voigt et al.*, 2004; *Wilmsen et al.*, 2007; *Kuhnt et al.*, 2009]. The mid-Cenomanian glaciation hypothesis was contradicted by a rigorous foraminiferal stable isotopic study that demonstrated the absence of a coupled surface-and-deep $\delta^{18}O$ shift at the interval of a maximum sea level fall [*Ando et al.*, 2009a]. Our new foraminiferal $\delta^{18}O$ data from Tanzania can establish that a cooler climate mode was unlikely for the Cenomanian.

It should be noted that there are two contrasting long-term paleotemperature proxies suggesting that the oceans were cooler during the early to middle Cenomanian: (1) a global benthic foraminiferal $\delta^{18}O$ compilation [*Friedrich et al.*, 2012] and (2) an organic geochemical TEX_{86} index [*Forster et al.*, 2007a]. As for the former, the illustrated early-middle Cenomanian lowering of deepwater paleotemperatures [*Friedrich et al.*, 2012] can be regarded as an artifact of data availability, such that the $\delta^{18}O$ data used for this interval are solely from a single relatively deep site (ODP Site 1050; middle-lower bathyal transition). As for the latter, the TEX_{86} profile is from ODP Site 1258, Demerara Rise, wherein early-middle Cenomanian strengthening of the upper ocean current is inferred from a temporarily greater vertical gradient of Nd isotopes [*Jiménez Berrocoso et al.*, 2010a]. This fact may point to a possibility that the reported cooler TEX_{86} temperatures are regional in scale and better explained by the overturning of cooler subsurface waters [e.g., *Tierney*, 2012] than by global climatic factors.

A limitation of our TDP Site 24 study is the unavailability of $\delta^{18}O$ data for the final 2.0 Myr of the Cenomanian. This limitation precludes testing of a proposed latest Cenomanian extreme warming event [*Huber et al.*, 2002; *Gustafsson et al.*, 2003], which may have preconditioned Earth's surface environments for the C/T Oceanic Anoxic Event [*Ando et al.*, 2009b]. Discovery of a sequence yielding exquisitely preserved foraminifera across this short period is anticipated to test the likelihood of a latest Cenomanian-earliest Turonian extra hyperthermal event superimposed on the background hot greenhouse conditions.

6.2. Uncertain Timing of Transition Into Mid-Cretaceous Hot Greenhouse

Accepting the new view from Tanzania of the extremely warm early Cenomanian climate, the duration of the mid-Cretaceous hot greenhouse can be extended to the latest Albian. This is because similar $\delta^{18}O$ results of exceptionally well-preserved foraminifera are reported from ODP Site 1052, Blake Nose, western North Atlantic (Albian paleolatitude = ~25°N; paleodepth = upper bathyal) [*Wilson and Norris*, 2001; *Petrizzo et al.*, 2008], supporting significant warmth during the latest Albian. There, the average planktonic foraminiferal $\delta^{18}O$ value is higher than at TDP Site 24 by ~+1‰, yet both sites are nearly symmetrically positioned relative to the paleoequator. The discrepancy in $\delta^{18}O$ at the open-ocean midlatitude Northern vs. Southern Hemispheres can be accounted for by more ^{18}O-enriched North Atlantic surface seawater during the mid-Cretaceous [*Zhou et al.*, 2008].

By extending the duration of the hot greenhouse back to the latest Albian, a question emerges as to when exactly was the critical transition into the hot greenhouse mode within the mid-Cretaceous greenhouse. There is growing evidence that after the initial warming pulse during the early Aptian [e.g., *Ando et al.*, 2008; *Mutterlose et al.*, 2014], the late Aptian was a demonstrably cooler period than other times in the mid-Cretaceous [*Clarke and Jenkyns*, 1999; *Maurer et al.*, 2013; *McAnena et al.*, 2013]. If these paleoenvironmental reconstructions are reliable, then the critical paleoclimatic transition from a "cool greenhouse" to the hot greenhouse should have occurred after the late Aptian and before the latest Albian (~113–103 Ma).

The possibility that the late Aptian cooling persisted into the early Albian emerges from another detailed Blake Nose $\delta^{18}O$ data set of very well preserved foraminifera from ODP Site 1049 by *Huber et al.* [2011]. On the one hand, the $\delta^{18}O$-based surface temperatures from planktonic foraminifera are unusually low for such a subtropical setting, necessitating explanations based on remarkable local anomalies in evaporation and salinity [*Huber et al.*, 2011]. On the other hand, the Site 1049 benthic foraminiferal $\delta^{18}O$ data are consistent and appear reasonable, with values comparable with global deep-sea benthic $\delta^{18}O$ records of the latest Cretaceous (Campanian-Maastrichtian) cool greenhouse [e.g., *Huber et al.*, 2002; *Ando et al.*, 2013]. There exists a slight negative $\delta^{18}O$ shift from the latest Aptian through the early Albian [*Huber et al.*, 2011], which may point to a gradual long-term increase in bottom-water temperature. For establishing such benthic paleotemperature interpretations, though, it is necessary to properly constrain the deep-water $\delta^{18}O$ composition of the proto-North Atlantic basin, which seems to be a challenging issue due to the restricted basin configuration.

In any case, the lack of reliable foraminiferal $\delta^{18}O$ data is apparent for much of the Albian. One exceptional data source may be the benthic foraminiferal $\delta^{18}O$ record from DSDP Site 511, Falkland Plateau, South Atlantic (paleolatitude = ~60°S). This site is important in that the stratigraphic coverage spans most of the Albian interval, providing key information on Albian high-latitude calcareous microfossil fauna, biostratigraphy, and evolution, and also serving as one of reference sections for the standard mid-Cretaceous strontium isotope curve [*Huber et al.*, 1995, 2002; *Bralower et al.*, 1997; *Fassell and Bralower*, 1999; *Huber and Leckie*, 2011]. Difficulties in interpreting the Albian part of Site 511 foraminiferal $\delta^{18}O$ data arise from the depositional setting which was possibly as shallow as middle neritic, judging from the intense bioturbation, molluscan-rich biofacies with solitary corals, and the benthic foraminiferal assemblage [*Jeletzky*, 1983; *Basov and Krasheninnikov*, 1983; *Shipboard Scientific Party*, 1983; see also *Fassell and Bralower*, 1999, p. 122 therein]. Such a setting would be difficult to compare with the slope to abyssal mid-Cretaceous sites previously studied for benthic $\delta^{18}O$ paleotemperatures. Also, this South Atlantic site might have had peculiar paleoceanographic conditions with a more restricted paleogeography during the Albian, which may be relevant to the predominance of opportunistic hedbergellid species of planktonic foraminifera [*Huber et al.*, 1995; *Huber and Leckie*, 2011].

In summary, subsequent to a relatively cool greenhouse mode during the late Aptian (and/or early Albian), the mid-Cretaceous hot greenhouse should have been established by the latest Albian. Still, the precise timing and tempo of this critical paleoclimatic transition cannot be constrained by existing $\delta^{18}O$ data, and so no inference can be made on the ultimate trigger(s), sustaining mechanism(s), and paleoenvironmental and biotic consequences of this major yet hitherto unexplored global change during the mid-Cretaceous. The key to advancing this field of paleoclimatology is the discovery of stratigraphically expanded and continuous, well-dated, paleoceanographically uncompromised Albian hemipelagic site(s) with ubiquitous occurrence of exceptionally well-preserved foraminifera.

7. Conclusions

We have presented a new Tanzanian early Cenomanian stable isotope data set of exceptionally well-preserved foraminifera and discussed its significance relative to the existence and duration of a "hot greenhouse" mode within the normal mid-Cretaceous greenhouse. The stratigraphic interval analyzed at TDP Site 24 consists of a thick (~50 m) sequence of upper bathyal interbedded siltstones and fine-grained sandstones. Numerical age for this interval spans 99.9–95.9 Ma based on the biostratigraphy and biochronology of planktonic foraminifera (*Th. globotruncanoides* Zone) and nannofossils (*C. kennedyi* to *L. eccentricus* Zones; the latter tentatively proposed in this study). Both $\delta^{18}O$ data series of exceptionally well-preserved planktonic foraminifera (*Pg. stephani* and *Th. globotruncanoides*) and benthic foraminifera (*Lenticulina* spp.) are surprisingly consistent at

−4.3‰ and at −1.9‰, respectively, suggesting very high and stable marine paleotemperatures offshore Tanzania (~40°S paleolatitude) during the early Cenomanian. Paleotemperatures (conservative estimates) were likely >31°C at the surface and >17°C at the seafloor. These water-column paleotemperature ranges for the southern midlatitudes are higher than those in the latest GCM mid-Cretaceous simulation [*Zhou et al.*, 2008] but are very similar to the recent hot greenhouse reconstructions from Turonian TDP sites [*MacLeod et al.*, 2013]. It is highly probable, despite a lack of data from the final 2.0 Myr interval, that the Cenomanian was a period of sustained hot greenhouse conditions. This paleoclimate mode may extend back to the latest Albian with consideration of comparable $\delta^{18}O$ data sets from Blake Nose, western North Atlantic [*Wilson and Norris*, 2001; *Petrizzo et al.*, 2008]. By integrating other sources of mid-Cretaceous paleoclimate indicators, the critical transition into the observed hot greenhouse mode from the background normal (cool) greenhouse conditions can be predicted to have occurred after the late Aptian (and/or early Albian) and prior to the latest Albian, but the precise timing remains uncertain.

Acknowledgments

Biostratigraphic and numerical data supporting Figures 2 and 5 are available as Tables S1 and S2 of the supporting information. Funding was provided by the National Science Foundation (NSF EAR 0641956 to MacLeod and Huber) and the Smithsonian Institution's Walcott Fund (to Huber). The senior author (Ando) gratefully acknowledges funding supports from a Visiting Scientist fellowship from the National Museum of Natural History, Smithsonian Institution, and partly from the W. Storrs Cole Award from the Geological Society of America and the Cushman Foundation. We are grateful for the generous assistance of staff from the Tanzanian Development Petroleum Corporation, including Joyce Singano, Michael Kereme, Ephrem Mchana, Amina Mweneinda, and Emma Msaki, and the Tanzania Commission for Science and Technology. We also thank Álvaro Jiménez Berrocoso for provision of the source graphic file for TDP Site 24 lithostratigraphy and Ines Wendler for suggestions for benthic foraminiferal identifications. Constructive reviews from R. Mark Leckie and Paul Pearson are highly appreciated.

References

Ando, A., K. Kaiho, H. Kawahata, and T. Kakegawa (2008), Timing and magnitude of early Aptian extreme warming: Unraveling primary $\delta^{18}O$ variation in indurated pelagic carbonates at Deep Sea Drilling Project Site 463, central Pacific Ocean, *Palaeogeogr. Palaeoclimatol. Palaeoecol.*, *260*, 463–476, doi:10.1016/j.palaeo.2007.12.007.

Ando, A., B. T. Huber, K. G. MacLeod, T. Ohta, and B.-K. Khim (2009a), Blake Nose stable isotopic evidence against the mid-Cenomanian glaciation hypothesis, *Geology*, *37*, 451–454, doi:10.1130/G25580A.1.

Ando, A., T. Nakano, K. Kaiho, T. Kobayashi, E. Kokado, and B.-K. Khim (2009b), Onset of seawater $^{87}Sr/^{86}Sr$ excursion prior to Cenomanian–Turonian Oceanic Anoxic Event 2? New Late Cretaceous strontium isotope curve from the central Pacific Ocean, *J. Foraminiferal Res.*, *39*, 322–334, doi:10.2113/gsjfr.39.4.322.

Ando, A., B. T. Huber, and K. G. MacLeod (2010), Depth-habitat reorganization of planktonic foraminifera across the Albian/Cenomanian boundary, *Paleobiology*, *36*, 357–373, doi:10.1666/09027.1.

Ando, A., S. C. Woodard, H. F. Evans, K. Littler, S. Herrmann, K. G. MacLeod, S. Kim, B.-K. Khim, S. A. Robinson, and B. T. Huber (2013), An emerging palaeoceanographic 'missing link': Multidisciplinary study of rarely recovered parts of deep-sea Santonian–Campanian transition from Shatsky Rise, *J. Geol. Soc.*, *170*, 381–384, doi:10.1144/jgs2012-137.

Aze, T., et al. (2014), Extreme warming of tropical waters during the Paleocene–Eocene Thermal Maximum, *Geology*, *42*, 739–742, doi:10.1130/G35637.1.

Barrera, E., B. T. Huber, S. M. Savin, and P.-N. Webb (1987), Antarctic marine temperatures: Late Campanian through early Paleocene, *Paleoceanography*, *2*, 21–47, doi:10.1029/PA002i001p00021.

Barron, E. J., and W. M. Washington (1985), Warm Cretaceous climates: High atmospheric CO_2 as a plausible mechanism, in *The Carbon Cycle and Atmospheric CO_2: Natural Variations Archean to Present*, *Geophys. Monogr.*, vol. 32, edited by E. T. Sundquist and W. S. Broecker, pp. 546–553, AGU, Washington, D. C.

Basov, I. A., and V. A. Krasheninnikov (1983), Benthic foraminifers in Mesozoic and Cenozoic sediments of the southwestern Atlantic as an indicator of paleoenvironment, Deep Sea Drilling Project Leg 71, *Initial Rep. Deep Sea Drill. Program*, *71*, 739–787, doi:10.2973/dsdp.proc.71.128.1983.

Bemis, B. E., H. J. Spero, J. Bijma, and D. W. Lea (1998), Reevaluation of the oxygen isotopic composition of planktonic foraminifera: Experimental results and revised paleotemperature equations, *Paleoceanography*, *13*, 150–160, doi:10.1029/98PA00070.

Bice, K. L., B. T. Huber, and R. D. Norris (2003), Extreme polar warmth during the Cretaceous greenhouse? Paradox of the late Turonian $\delta^{18}O$ record at Deep Sea Drilling Project Site 511, *Paleoceanography*, *18*(2), 1031, doi:10.1029/2002PA000848.

Birch, H., H. K. Coxall, P. N. Pearson, D. Kroon, and M. O'Regan (2013), Planktonic foraminifera stable isotopes and water column structure: Disentangling ecological signals, *Mar. Micropaleontol.*, *101*, 127–145, doi:10.1016/j.marmicro.2013.02.002.

Bornemann, A., R. D. Norris, O. Friedrich, B. Beckmann, S. Schouten, J. S. Sinninghe Damsté, J. Vogel, P. Hofmann, and T. Wagner (2008), Isotopic evidence for glaciation during the Cretaceous supergreenhouse, *Science*, *319*, 189–192, doi:10.1126/science.1148777.

Bralower, T. J., P. D. Fullagar, C. K. Paull, G. S. Dwyer, and R. M. Leckie (1997), Mid-Cretaceous strontium-isotope stratigraphy of deep-sea sections, *Geol. Soc. Am. Bull.*, *109*, 1421–1442, doi:10.1130/0016-7606(1997)109<1421:MCSISO>2.3.CO;2.

Burnett, J. A. (1998), Upper Cretaceous, in *Calcareous Nannofossil Biostratigraphy*, edited by P. R. Bown, pp. 132–199, Kluwer Acad, Dordrecht.

Caldeira, K., and M. R. Rampino (1991), The mid-Cretaceous super plume, carbon dioxide, and global warming, *Geophys. Res. Lett.*, *18*, 987–990, doi:10.1029/91GL01237.

Clarke, L. J., and H. C. Jenkyns (1999), New oxygen isotope evidence for long-term Cretaceous climatic change in the Southern Hemisphere, *Geology*, *27*, 699–702, doi:10.1130/0091-7613(1999)027<0699:NOIEFL>2.3.CO;2.

Corbett, M. J., D. K. Watkins, and J. J. Pospichal (2014), A quantitative analysis of calcareous nannofossil bioevents of the Late Cretaceous (Late Cenomanian–Coniacian) Western Interior Seaway and their reliability in established zonation schemes, *Mar. Micropaleontol.*, *109*, 30–45, doi:10.1016/j.marmicro.2014.04.002.

Cramer, B. S., K. G. Miller, P. J. Barrett, and J. D. Wright (2011), Late Cretaceous–Neogene trends in deep ocean temperature and continental ice volume: Reconciling records of benthic foraminiferal geochemistry ($\delta^{18}O$ and Mg/Ca) with sea level history, *J. Geophys. Res.*, *116*, C12023, doi:10.1029/2011JC007255.

de Nooijer, L. J., T. Toyofuku, and H. Kitazato (2009), Foraminifera promote calcification by elevating their intracellular pH, *Proc. Natl. Acad. Sci. U.S.A.*, *106*, 15,374–15,378, doi:10.1073/pnas.0904306106.

Erbacher, J., O. Friedrich, P. A. Wilson, J. Lehmann, and W. Weiss (2011), Short-term warming events during the boreal Albian (mid-Cretaceous), *Geology*, *39*, 223–226, doi:10.1130/G31606.1.

Fassell, M. L., and T. J. Bralower (1999), Warm, equable mid-Cretaceous: Stable isotope evidence, in *Evolution of the Cretaceous Ocean-Climate System*, edited by E. Barrera and C. C. Johnson, *Geol. Soc. Am. Spec. Publ.*, *332*, 121–142.

Forster, A., S. Schouten, M. Baas, and J. S. Sinninghe Damsté (2007a), Mid-Cretaceous (Albian–Santonian) sea surface temperature record of the tropical Atlantic Ocean, *Geology*, *35*, 919–922, doi:10.1130/G23874A.1.

Forster, A., S. Schouten, K. Moriya, P. A. Wilson, and J. S. Sinninghe Damsté (2007b), Tropical warming and intermittent cooling during the Cenomanian/Turonian oceanic anoxic event 2: Sea surface temperature records from the equatorial Atlantic, *Paleoceanography*, *22*, PA1219, doi:10.1029/2006PA001349.

Friedrich, O., G. Schmiedl, and H. Erlenkeuser (2006), Stable isotope composition of Late Cretaceous benthic foraminifera from the southern South Atlantic: Biological and environmental effects, *Mar. Micropaleontol.*, *58*, 135–157, doi:10.1016/j.marmicro.2005.10.005.

Friedrich, O., J. Erbacher, K. Moriya, P. A. Wilson, and H. Kunhert (2008), Warm saline intermediate waters in the Cretaceous tropical Atlantic Ocean, *Nat. Geosci.*, *1*, 453–457, doi:10.1038/ngeo217.

Friedrich, O., R. D. Norris, and J. Erbacher (2012), Evolution of middle to Late Cretaceous oceans—A 55 m.y. record of Earth's temperature and carbon cycle, *Geology*, *40*, 107–110, doi:10.1130/G32701.1.

Gale, A. S., J. Hardenbol, B. Hathway, W. J. Kennedy, J. R. Young, and V. Phansalkar (2002), Global correlation of Cenomanian (Upper Cretaceous) sequences: Evidence for Milankovitch control on sea level, *Geology*, *30*, 291–294, doi:10.1130/0091-7613(2002)030<0291:GCOCUC>2.0.CO;2.

Gale, A. S., S. Voigt, B. B. Sageman, and W. J. Kennedy (2008), Eustatic sea-level record for the Cenomanian (Late Cretaceous)—Extension to the Western Interior Basin, USA, *Geology*, *36*, 859–862, doi:10.1130/G24838A.1.

Georgescu, M. D., and B. T. Huber (2006), *Paracostellagerina* nov. gen., a meridionally costellate planktonic foraminiferal genus of the middle Cretaceous (latest Albian-earliest Cenomanian), *J. Foraminiferal Res.*, *36*, 368–373, doi:10.2113/gsjfr.36.4.368.

Grossman, E. L. (2012), Applying oxygen isotope paleothermometry in deep time, in *Reconstructing Earth's Deep-Time Climate—The State of the Art in 2012*, edited by L. C. Ivany and B. T. Huber, *Paleontol. Soc. Pap.*, *18*, 39–67.

Gruber, N., and C. D. Keeling (2001), An improved estimate of the isotopic air-sea disequilibrium of CO_2: Implications for the oceanic uptake of anthropogenic CO_2, *Geophys. Res. Lett.*, *28*, 555–558, doi:10.1029/2000GL011853.

Gustafsson, M., A. Holbourn, and W. Kuhnt (2003), Changes in Northeast Atlantic temperature and carbon flux during the Cenomanian/Turonian paleoceanographic event: The Goban Spur stable isotope record, *Palaeogeogr. Palaeoclimatol. Palaeoecol.*, *201*, 51–66, doi:10.1016/S0031-0182(03)00509-1.

Hay, W. W. (2008), Evolving ideas about the Cretaceous climate and ocean circulation, *Cretaceous Res.*, *29*, 725–753, doi:10.1016/j.cretres.2008.05.025.

Hay, W. W., et al. (1999), Alternative global Cretaceous paleogeography, in *Evolution of the Cretaceous Ocean-Climate System*, edited by E. Barrera and C. C. Johnson, *Geol. Soc. Am. Spec. Publ.*, *332*, 1–47

Huber, B. T., and R. M. Leckie (2011), Planktonic foraminiferal species turnover across deep-sea Aptian/Albian boundary sections, *J. Foraminiferal Res.*, *41*, 53–95, doi:10.2113/gsjfr.41.1.53.

Huber, B. T., D. A. Hodell, and C. P. Hamilton (1995), Middle–Late Cretaceous climate of the southern high latitudes: Stable isotopic evidence for minimal equator-to-pole thermal gradients, *Geol. Soc. Am. Bull.*, *107*, 1164–1191, doi:10.1130/0016-7606(1995)107<1164:MLCCOT>2.3.CO;2.

Huber, B. T., R. D. Norris, and K. G. MacLeod (2002), Deep-sea paleotemperature record of extreme warmth during the Cretaceous, *Geology*, *30*, 123–126, doi:10.1130/0091-7613(2002)030<0123:DSPROE>2.0.CO;2.

Huber, B. T., K. G. MacLeod, D. R. Gröcke, and M. Kucera (2011), Paleotemperature and paleosalinity inferences and chemostratigraphy across the Aptian/Albian boundary in the subtropical North Atlantic, *Paleoceanography*, *26*, PA4221, doi:10.1029/2011PA002178.

Hut, G. (1987), Consultants' group meeting on stable isotope reference samples for geochemical and hydrological investigations, IAEA, Vienna, 16–18 September 1985. International Atomic Energy Agency.

Jaffrés, J. B. D., G. A. Shields, and K. Wallmann (2007), The oxygen isotope evolution of seawater: A critical review of a long-standing controversy and an improved geological water cycle model for the past 3.4 billion years, *Earth Sci. Rev.*, *83*, 83–122, doi:10.1016/j.earscirev.2007.04.002.

Jeletzky, J. A. (1983), Macroinvertebrate paleontology, biochronology, and paleoenvironments of Lower Cretaceous and Upper Jurassic rocks, Deep Sea Drilling Hole 511, eastern Falkland Plateau, *Initial Rep. Deep Sea Drill. Program*, *71*, 951–975, doi:10.2973/dsdp.proc.71.135.1983.

Jiménez Berrocoso, Á., K. G. MacLeod, E. E. Martin, E. Bourbon, C. Isaza Londoño, and C. Basak (2010a), Nutrient trap for Late Cretaceous organic-rich black shales in the tropical North Atlantic, *Geology*, *38*, 1111–1114, doi:10.1130/G31195.1.

Jiménez Berrocoso, Á., K. G. MacLeod, B. T. Huber, J. A. Lees, I. Wendler, P. R. Bown, A. K. Mweneinda, C. Isaza Londoño, and J. M. Singano (2010b), Lithostratigraphy, biostratigraphy and chemostratigraphy of Upper Cretaceous sediments from southern Tanzania: Tanzania drilling project sites 21–26, *J. Afr. Earth Sci.*, *57*, 47–69, doi:10.1016/j.jafrearsci.2009.07.010.

Jiménez Berrocoso, Á., et al. (2012), Lithostratigraphy, biostratigraphy and chemostratigraphy of Upper Cretaceous and Paleogene sediments from southern Tanzania: Tanzania Drilling Project Sites 27–35, *J. Afr. Earth Sci.*, *70*, 36–57, doi:10.1016/j.jafrearsci.2012.05.006.

Jiménez Berrocoso, Á., et al. (2015), The Lindi Formation (upper Albian–Coniacian) and Tanzania Drilling Project Sites 36–40 (Lower Cretaceous to Paleogene): Lithostratigraphy, biostratigraphy and chemostratigraphy, *J. Afr. Earth Sci.*, *101*, 282–308, doi:10.1016/j.jafrearsci.2014.09.017.

Johnson, C. C., E. J. Barron, E. G. Kauffman, M. A. Arthur, P. J. Fawcett, and M. K. Yasuda (1996), Middle Cretaceous reef collapse linked to ocean heat transport, *Geology*, *24*, 376–380, doi:10.1130/0091-7613(1996)024<0376:MCRCLT>2.3.CO;2.

Katz, M. E., D. R. Katz, J. D. Wright, K. G. Miller, D. K. Pak, N. J. Shackleton, and E. Thomas (2003), Early Cenozoic benthic foraminiferal isotopes: Species reliability and interspecies correction factors, *Paleoceanography*, *18*(2), 1024, doi:10.1029/2002PA000798.

Kendall, C., and T. B. Coplen (2001), Distribution of oxygen-18 and deuterium in river waters across the United States, *Hydrol. Process.*, *15*, 1363–1393, doi:10.1002/hyp.217.

Kennedy, W. J., A. S. Gale, J. A. Lees, and M. Caron (2004), The Global Boundary Stratotype Section and Point (GSSP) for the base of the Cenomanian Stage, Mont Risou, Hautes-Alpes, France, *Episodes*, *27*, 21–32.

Kent, P. E., J. A. Hunt, and D. W. Johnstone (1971), *The Geology and Geophysics of Coastal Tanzania*, *Inst. Geol. Sci. Geophys. Pap.*, vol. 6, HMSO, London.

Kim, S.-T., and J. R. O'Neil (1997), Equilibrium and nonequilibrium oxygen isotope effects in synthetic carbonates, *Geochim. Cosmochim. Acta*, *61*, 3461–3475, doi:10.1016/S0016-7037(97)00169-5.

Kuhnt, W., A. Holbourn, A. Gale, E. H. Chellai, and W. J. Kennedy (2009), Cenomanian sequence stratigraphy and sea-level fluctuations in the Tarfaya Basin (SW Morocco), *Geol. Soc. Am. Bull.*, *121*, 1695–1710, doi:10.1130/B26418.1.

Larson, R. L. (1991a), Latest pulse of Earth: Evidence for a mid-Cretaceous superplume, *Geology*, *19*, 547–550, doi:10.1130/0091-7613(1991)019<0547:LPOEEF>2.3.CO;2.

Larson, R. L. (1991b), Geological consequences of superplumes, *Geology*, *19*, 963–966, doi:10.1130/0091-7613(1991)019<0963:GCOS>2.3.CO;2.

Leckie, R. M. (1984), Mid-Cretaceous planktonic foraminiferal biostratigraphy off central Morocco, Deep Sea Drilling Project Leg 79, Sites 545 and 547, *Initial Rep. Deep Sea Drill. Program*, *79*, 579–620, doi:10.2973/dsdp.proc.79.122.1984.

MacLeod, K. G., B. T. Huber, Á. Jiménez Berrocoso, and I. Wendler (2013), A stable and hot Turonian without glacial $\delta^{18}O$ excursions is indicated by exquisitely preserved Tanzanian foraminifera, *Geology*, *41*, 1083–1086, doi:10.1130/G34510.1.

Maurer, F., F. S. P. van Buchem, G. P. Eberli, B. J. Pierson, M. J. Raven, P.-H. Larsen, M. I. Al-Husseini, and B. Vincent (2013), Late Aptian long-lived glacio-eustatic lowstand recorded on the Arabian Plate, *Terra Nova*, *25*, 87–94, doi:10.1111/ter.12009.

McAnena, A., S. Flögel, P. Hofmann, J. O. Herrle, A. Griesand, J. Pross, H. M. Talbot, J. Rethemeyer, K. Wallmann, and T. Wagner (2013), Atlantic cooling associated with a marine biotic crisis during the mid-Cretaceous period, *Nat. Geosci.*, *6*, 558–561, doi:10.1038/NGEO1850.

Miller, K. G., P. J. Sugarman, J. V. Browning, M. A. Kominz, J. C. Hernández, R. K. Olsson, J. D. Wright, M. D. Feigenson, and W. Van Sickel (2003), Late Cretaceous chronology of large, rapid sea-level changes: Glacioeustasy during the greenhouse world, *Geology*, *31*, 585–588, doi:10.1130/0091-7613(2003)031<0585:LCCOLR>2.0.CO;2.

Miller, K. G., J. D. Wright, and J. V. Browning (2005), Visions of ice sheets in a greenhouse world, *Mar. Geol.*, *217*, 215–231, doi:10.1016/j.margeo.2005.02.007.

Mitchell, S. F., C. R. C. Paul, and A. S. Gale (1996), Carbon isotopes and sequence stratigraphy, in *High Resolution Sequence Stratigraphy: Innovations and Applications*, edited by J. A. Howell and J. F. Aitken, *Geol. Soc. Spec. Publ.*, *104*, 11–24.

Moriya, K., P. A. Wilson, O. Friedrich, J. Erbacher, and H. Kawahata (2007), Testing for ice sheets during the mid-Cretaceous greenhouse using glassy foraminiferal calcite from the mid-Cenomanian tropics on Demerara Rise, *Geology*, *35*, 615–618, doi:10.1130/G23589A.1.

Mutterlose, J., C. Bottini, S. Schouten, and J. S. Sinninghe Damsté (2014), High sea-surface temperatures during the early Aptian Oceanic Anoxic Event 1a in the Boreal Realm, *Geology*, *42*, 439–442, doi:10.1130/G35394.1.

Nederbragt, A. J., A. Fiorentino, and B. Klosowska (2001), Quantitative analysis of calcareous microfossil across the Albian–Cenomanian boundary oceanic anoxic event at DSDP Site 547 (North Atlantic), *Palaeogeogr. Palaeoclimatol. Palaeoecol.*, *166*, 401–421, doi:10.1016/S0031-0182(00)00227-3.

Norris, R. D., and P. A. Wilson (1998), Low-latitude sea-surface temperatures for the mid-Cretaceous and the evolution of planktic foraminifera, *Geology*, *26*, 823–826, doi:10.1130/0091-7613(1998)026<0823:LLSSTF>2.3.CO;2.

Norris, R. D., K. L. Bice, E. A. Magno, and P. A. Wilson (2002), Jiggling the tropical thermostat in the Cretaceous hothouse, *Geology*, *30*, 299–302, doi:10.1130/0091-7613(2002)030<0299:JTTTIT>2.0.CO;2.

Ogg, J. G., and L. A. Hinnov (2012), Cretaceous, in *The Geologic Time Scale 2012*, edited by F. M. Gradstein et al., pp. 793–853, Elsevier B. V, Amsterdam.

Pearson, P. N. (2012), Oxygen isotopes in foraminifera: Overview and historical review, in *Reconstructing Earth's Deep-Time Climate—The State of the Art in 2012*, edited by L. C. Ivany and B. T. Huber, *Paleontol. Soc. Pap.*, *18*, 1–38.

Pearson, P. N., P. W. Ditchfield, J. Singano, K. G. Harcourt-Brown, C. J. Nicholas, R. K. Olsson, N. J. Shackleton, and M. A. Hall (2001), Warm tropical sea surface temperatures in the Late Cretaceous and Eocene epochs, *Nature*, *413*, 481–487, doi:10.1038/35097000.

Perch-Nielsen, K. (1985), Mesozoic calcareous nannofossils, in *Plankton Stratigraphy*, edited by H. M. Bolli et al., pp. 329–426, Cambridge Univ. Press, Cambridge, U. K..

Petrizzo, M. R., B. T. Huber, P. A. Wilson, and K. G. MacLeod (2008), Late Albian paleoceanography of the western subtropical North Atlantic, *Paleoceanography*, *23*, PA1213, doi:10.1029/2007PA001517.

Poulsen, C. J., E. J. Barron, M. A. Arthur, and W. H. Peterson (2001), Response of the mid-Cretaceous global oceanic circulation to tectonic and CO_2 forcings, *Paleoceanography*, *16*, 576–592, doi:10.1029/2000PA000579.

Premoli Silva, I., and C. L. McNulty (1984), Planktonic foraminifers and calpionellids from Gulf of Mexico sites, Deep Sea Drilling Project Leg 77, *Initial Rep. Deep Sea Drill. Proj.*, *77*, 547–584, doi:10.2973/dsdp.proc.77.122.1984.

Robaszynski, F., M. Caron, F. Amédro, C. Dupuis, J. Hardenbol, J. M. González Donoso, D. Linares, and S. Gartner (1993), Le Cénomanien de la région de Kalaat Senan (Tunisie centrale): Litho-biostratigraphie et interprétation séquentielle, *Rev. Paléobiol.*, *12*, 351–505.

Roberts, C. D., A. N. Legrande, and A. K. Tripati (2011), Sensitivity of seawater oxygen isotopes to climatic and tectonic boundary conditions in an early Paleogene simulation with GISS ModelE-R, *Paleoceanography*, *26*, PA4203, doi:10.1029/2010PA002025.

Royer, D. L., R. A. Berner, I. P. Montañez, N. J. Tabor, and D. J. Beerling (2004), CO_2 as a primary driver of Phanerozoic climate, *GSA Today*, *14*, 4–10, doi:10.1130/1052-5173(2004)014<4:CAAPDO>2.0.CO;2.

Scotese, C. R. (2004), A continental drift flipbook, *J. Geol.*, *112*, 729–741, doi:10.1086/424867.

Sewall, J. O., R. S. W. van de Wal, K. van der Zwan, C. van Oosterhout, H. A. Dijkstra, and C. R. Scotese (2007), Climate model boundary conditions for four Cretaceous time slices, *Clim. Past*, *3*, 647–657, doi:10.5194/cp-3-647-2007.

Shackleton, N. J., and J. P. Kennett (1975), Paleotemperature history of the Cenozoic and the initiation of Antarctic glaciation: Oxygen and carbon isotope analyses in DSDP Sites 277, 279, and 281, *Initial Rep. Deep Sea Drill. Program*, *29*, 743–755, doi:10.2973/dsdp.proc.29.117.1975.

Shipboard Scientific Party (1983), Site 511, *Initial Rep. Deep Sea Drill. Proj.*, *71*, 21–109, doi:10.2973/dsdp.proc.71.102.1983.

Sikora, P. J., and R. K. Olsson (1991), A paleoslope model of late Albian to early Turonian foraminifera of the western Atlantic margin and North Atlantic basin, *Mar. Micropaleontol.*, *18*, 25–72, doi:10.1016/0377-8398(91)90005-Q.

Spero, H. J., J. Bijma, D. W. Lea, and B. E. Bemis (1997), Effect of seawater carbonate concentration on foraminiferal carbon and oxygen isotopes, *Nature*, *390*, 497–500, doi:10.1038/37333.

Strauss, J., E. L. Grossman, and S. F. DiMarco (2012), Stable isotope characterization of hypoxia-susceptible waters on the Louisiana shelf: Tracing freshwater discharge and benthic respiration, *Cont. Shelf Res.*, *47*, 7–15, doi:10.1016/j.csr.2012.07.020.

Tierney, J. E. (2012), GDGT thermometry: Lipid tools for reconstructing paleotemperatures, in *Reconstructing Earth's Deep-Time Climate—The State of the Art in 2012*, *Paleontol. Soc. Pap.*, vol. 18, edited by L. C. Ivany and B. T. Huber, pp. 115–131.

Tindall, J., R. Flecker, P. Valdes, D. N. Schmidt, P. Markwick, and J. Harris (2010), Modelling the oxygen isotope distribution of ancient seawater using a coupled ocean–atmosphere GCM: Implications for reconstructing early Eocene climate, *Earth Planet. Sci. Lett.*, *292*, 265–273, doi:10.1016/j.epsl.2009.12.049.

Veizer, J., and A. Prokoph (2015), Temperatures and oxygen isotopic composition of Phanerozoic oceans, *Earth Sci. Rev.*, *146*, 92–104, doi:10.1016/j.earscirev.2015.03.008.

Veizer, J., et al. (1999), $^{87}Sr/^{86}Sr$, $\delta^{13}C$ and $\delta^{18}O$ evolution of Phanerozoic seawater, *Chem. Geol.*, *161*, 59–88, doi:10.1016/S0009-2541(99)00081-9.

Veizer, J., Y. Godderis, and L. M. François (2000), Evidence for decoupling of atmospheric CO_2 and global climate during the Phanerozoic eon, *Nature*, *408*, 698–701, doi:10.1038/35047044.

Voigt, S., A. S. Gale, and S. Flögel (2004), Midlatitude shelf seas in the Cenomanian-Turonian greenhouse world: Temperature evolution and North Atlantic circulation, *Paleoceanography*, *19*, PA4020, doi:10.1029/2004PA001015.

Wagner, A. J., and N. C. Slowey (2011), Oxygen isotopes in seawater from the Texas-Louisiana shelf, *Bull. Mar. Sci.*, *87*, 1–12, doi:10.5343/bms.2010.1004.

Wallmann, K. (2004), Impact of atmospheric CO_2 and galactic cosmic radiation on Phanerozoic climate change and the marine $\delta^{18}O$ record, *Geochem. Geophys. Geosyst.*, *5*, Q06004, doi:10.1029/2003GC000683.

Watkins, D. K., and J. L. Bowdler (1984), Cretaceous calcareous nannofossils from Deep Sea Drilling Project Leg 77, Southeast Gulf of Mexico, *Initial Rep. Deep Sea Drill. Program*, *77*, 649–674, doi:10.2973/dsdp.proc.77.127.1984.

Watkins, D. K., M. J. Cooper, and P. A. Wilson (2005), Calcareous nannoplankton response to late Albian Oceanic Anoxic Event 1d in the western North Atlantic, *Paleoceanography*, *20*, PA2010, doi:10.1029/2004PA001097.

Wendler, I., B. T. Huber, K. G. MacLeod, and J. E. Wendler (2013), Stable oxygen and carbon isotope systematics of exquisitely preserved Turonian foraminifera from Tanzania—Understanding isotopic signatures in fossils, *Mar. Micropaleontol.*, *102*, 1–33, doi:10.1016/j.marmicro.2013.04.003.

Wiegand, G. E. (1984), Cretaceous nannofossils from the Northwest African margin, Deep Sea Drilling Project Leg 79, *Initial Rep. Deep Sea Drill. Program*, *79*, 563–578, doi:10.2973/dsdp.proc.79.121.1984.

Wilmsen, M., B. Niebuhr, C. J. Wood, and D. Zawischa (2007), Fauna and palaeoecology of the Middle Cenomanian *Praeactinocamax primus* Event at the type locality, Wunstorf quarry, northern Germany, *Cretaceous Res.*, *28*, 428–460, doi:10.1016/j.cretres.2006.07.004.

Wilson, P. A., and R. D. Norris (2001), Warm tropical ocean surface and global anoxia during the mid-Cretaceous period, *Nature*, *412*, 425–429, doi:10.1038/35086553.

Wilson, P. A., R. D. Norris, and M. J. Cooper (2002), Testing the Cretaceous greenhouse hypothesis using glassy foraminiferal calcite from the core of the Turonian tropics on Demerara Rise, *Geology*, *30*, 607–610, doi:10.1130/0091-7613(2002)030<0607:TTCGHU>2.0.CO;2.

Zachos, J. C., L. D. Stott, and K. C. Lohmann (1994), Evolution of early Cenozoic marine temperatures, *Paleoceanography*, *9*, 353–387, doi:10.1029/93PA03266.

Zeebe, R. E. (2001), Seawater pH and isotopic paleotemperatures of Cretaceous oceans, *Palaeogeogr. Palaeoclimatol. Palaeoecol.*, *170*, 49–57, doi:10.1016/S0031-0182(01)00226-7.

Zeebe, R. E. (2012), History of seawater carbonate chemistry, atmospheric CO_2, and ocean acidification, *Annu. Rev. Earth Planet. Sci.*, *40*, 141–165, doi:10.1146/annurev-earth-042711-105521.

Zhou, J., C. J. Poulsen, D. Pollard, and T. S. White (2008), Simulation of modern and middle Cretaceous marine $\delta^{18}O$ with an ocean–atmosphere general circulation model, *Paleoceanography*, *23*, PA3223, doi:10.1029/2008PA001596.